International Journal of Applied Research 2015; 1(7): 69-74

ISSN Print: 2394-7500
ISSN Online: 2394-5869
Impact Factor: 5.2
IJAR 2015; 1(7): 69-74
www.allresearchjournal.com
Received: 06-04-2015
Accepted: 23-05-2015

Manish Garg
Department of Physics, S. D. College, Barnala-148101, Punjab, India.

Correspondence:
Manish Garg
Department of Physics, S. D. College, Barnala-148101, Punjab, India.

Linear and Non-linear analysis of distribution of reinforcement gradient in Functionally Graded Material Cylinder

Manish Garg

Abstract
This paper investigates the creep analysis of linear and non-linear distribution of SiC_P content in the cylinder made of functionally graded material and subjected to internal pressure. The creep behaviour of the composite cylinder is described by a Norton's Power law. The study reveals that for the linear and non-linear particle gradient, the radial stress decreases over the entire cylinder. By increasing Particle gradient in the FGM Linear and FGM Non-Linear Cylinders, the tangential stress increases near the inner radius but decreases toward the outer radius when compared with a similar cylinder but having uniform particle gradient. The magnitude of strain rates in functionally graded composite cylinder reduces significantly in the presence of non-linear SiC_P gradient along the radial direction.

Keywords: Functionally Graded Material, Pressure, Cylinder, Creep.

1. Introduction
Functionally graded materials (FGM) are composite materials formed of two or more constituent phases with a continuously variable composition (Birman and Byrd, 2007) [6]. Functionally graded materials are used in modern technologies for structural components such as those used in nuclear, aircraft, space engineering and pressure vessels (Loghman *et al.* 2011, Arya and Bhatnagar 1976; Bhatnagar *et al.* 1980; Becht and Chen 2000) [12, 1, 5, 3]. In most of these applications, cylinder is subjected to severe mechanical and thermal loads, causing significant creep and reducing its service life (Gupta and Pathak, 2001, Hagihara and Miyazaki, 2008 and, Tachibana and Iyoku, 2004) [11, 10, 16].
Arya *et al.* (1983) [2] investigated non-steady state creep in a thin circular cylindrical shell made of homogeneous, incompressible and orthotropic material. The results indicate that the presence of anisotropy could lead to a better shell design with lower strains and longer service life. Obata and Noda (1994) [13] presented a solution scheme to estimate steady state thermal stresses in a FG hollow circular cylinder to obtain the optimal distribution of reinforcement under different thermal loads. Chen *et al.* (2002) [7] obtained analytical solution of axisymmetric thermo-elastic problem of uniformly heated, FG isotropic hollow cylinder. The exact solution was obtained by considering modulus of elasticity and coefficient of thermal expansion as a power law function of radial distance. The study indicates that for a homogeneous and isotropic cylinder, no stress occurs when it is subjected to uniform temperature. Abrinia *et al.* (2008) obtained analytical solution to obtain radial and circumferential stresses in a FG thick cylindrical vessel under the influence of internal pressure and temperature. The effect of non-homogenity in FG cylinder was analyzed in the context of achieving the lowest stress levels in the cylinder. Singh and Gupta (2011) [15] investigated the steady state creep in transversely isotropic functionally graded cylinder, operating under internal and external pressures has been described by a threshold stress based creep law. The effect of anisotropy on creep stresses and creep rates in the FGM cylinder has been analyzed and compared with an isotropic FGM cylinder. The study reveals that in an anisotropic FGM cylinder i.e. when α deviates from unity, radial and tangential stresses are marginally affected whereas axial and effective stresses are significantly affected as compared to those in an isotropic FGM cylinder. The strain rates as well as inhomogeneity

in strain rates in the FGM cylinder decrease significantly when α reduces from 1.3 to 0.7. In the light of above mentioned, it has been decided to investigate the creep behaviour in a linear and non-linear FGM cylinder consisting of SiC_p particles by using Norton Law.

2. Distribution of reinforcement

The distribution of SiC_p in the FGM cylinder decreases from the inner to outer radius. The amount (vol %) of SiC_P, V(r), at any radius *r,* is given by,

$$V(r) = V_{\max} - \frac{(V_{\max} - V_{\min})(r-a)^m}{(b-a)^m} \quad (1)$$

Where *m* is the gradation index and $V_{\max}$ and $V_{\min}$ are respectively the maximum and minimum content of SiC_P at the inner and the outer radii of the cylinder respectively. The values of *m* are chosen as 1 and 2 for linear and non-linear FGM cylinders respectively.

The average SiC_p content in the cylinder can be expressed as,

$$V_{avg} = \frac{\int_a^b 2\pi r l V(r)\,dr}{\pi(b^2-a^2)l} = \frac{\int_a^b 2rV(r)\,dr}{(b^2-a^2)} \quad (2)$$

Where *l* is the length of cylinder.

Substituting *V(r)* from Eq. (1) into Eq. (2) and integrating, we get,

$$V_{\min} = \frac{3(m^3+6m^2+11m+6)V_{avg}(b+a) - mV_{\max}[3(m+3)\{(m+1)b+(m+3)a\}]}{6\{(m+3)\{(m+1)b+a\}\}} \quad (3)$$

3. Creep law and parameters

The creep behavior of the FGM cylinder is described by Norton's power law as,

$$\dot{\varepsilon}_e = B\sigma_e^n \quad (4)$$

Where $\dot{\varepsilon}_e$ is the effective strain rate, σ_e is the effective stress, *B* and *n* are material parameters describing the creep performance in the cylinder.

It is evident from the study of Singh and Ray, 2001 [14] that the values of creep parameters *B* and *n* appearing in the Norton's law depend on the content of reinforcement, which vary with the radial distance.

$$B(r) = B_O\left[\frac{V(r)}{V_{avg}}\right]^{\phi} \quad (5) \text{ and}$$

$$n(r) = n_O\left[\frac{V(r)}{V_{avg}}\right]^{-\phi} \quad (6)$$

Where B_o and n_o are respectively the values of creep parameters *B* and *n* respectively and ϕ is the grading index. The values of B_o, n_o and ϕ are the taken from the study of Chen *et al.,* 2007.

Table 1: Values of Creep parameters Chen *et al.,* 2007

Creep parameters:
B_o=2.77 x 10^{-16} (MP^{-n}/h) and n = 3.75
Grading index ϕ = 0.7

4. Mathematical formulation

Consider a FGM thick-walled hollow cylinder with an inner radius *a* (10 mm) and outer radius *b* (20 mm) subjected to an internal and external pressures *p* (90 *MPa*) and *q* (0 *MPa*) respectively, as mentioned in fig. 1.

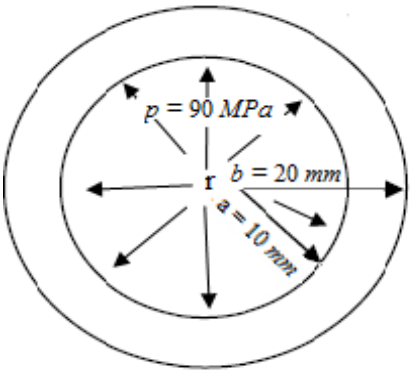

Fig 1: Diagram of the cylinder

The cylinder is made of isotropic material and is sufficiently long and hence is assumed under plain strain condition (i.e. axial strain rate, $\dot{\varepsilon}_z = 0$)

The radial ($\dot{\varepsilon}_r$) and tangential ($\dot{\varepsilon}_\theta$) strain rates in the cylinder are given by:

$$\dot{\varepsilon}_r = \frac{d\dot{u}_r}{dr} \quad (7) \text{ and}$$

$$\dot{\varepsilon}_\theta = \frac{\dot{u}_r}{r} \quad (8)$$

Where $\dot{u}_r = (du/dt)$ is the radial displacement rate and u is the radial displacement.

Eqs (7) and (8) may be solved to get the following compatibility equation,

$$r\frac{d\dot{\varepsilon}_\theta}{dr} = \dot{\varepsilon}_r - \dot{\varepsilon}_\theta \quad (9)$$

The cylinder is subjected to the following boundary conditions,

$$\sigma_r = -p \text{ at } r = a \quad (10)$$

$$\sigma_r = -q \text{ at } r = b \quad (11)$$

Where the negative sign of σ_r implies the compressive nature of radial stress.

By considering the equilibrium of forces acting on an element of the cylinder in the radial direction, we get,

$$r\frac{d\sigma_r}{dr} = \sigma_\theta - \sigma_r \quad (12)$$

The material of the cylinder is incompressible, therefore,

$$\dot{\varepsilon}_r + \dot{\varepsilon}_\theta + \dot{\varepsilon}_z = 0 \tag{13}$$

The constitutive equations under multi axial creep in an orthotropic cylinder, when the principal axes are the axes of reference, Bhatnagar and Gupta, 1969 [4] are given by,

$$\dot{\varepsilon}_r = \frac{\dot{\varepsilon}_e}{2\sigma_e}\left[2\sigma_r - \sigma_\theta - \sigma_z\right] \tag{14}$$

$$\dot{\varepsilon}_\theta = \frac{\dot{\varepsilon}_e}{2\sigma_e}\left[2\sigma_\theta - \sigma_z - \sigma_r\right] \tag{15}$$

$$\dot{\varepsilon}_z = \frac{\dot{\varepsilon}_e}{2\sigma_e}\left[2\sigma_z - \sigma_\theta - \sigma_r\right] \tag{16}$$

Where $\dot{\varepsilon}_e$ and σ_e are respectively the effective strain rate and effective stress in the FGM cylinder.

The von Mise's yield criterion, when the Principal axes of anisotropy are the axes of reference, Dieter, 1998 [9] is given by,

$$\sigma_e = \left[\frac{1}{2}\left\{(\sigma_\theta - \sigma_z)^2 + (\sigma_z - \sigma_r)^2 + (\sigma_r - \sigma_\theta)^2\right\}\right]^{1/2} \tag{17}$$

Since Under plain strain condition ($\dot{\varepsilon}_z = 0$), one may get from Eqs. (7), (8) and (13),

$$\dot{u}_r = \frac{C}{r} \tag{18}$$

Where C is a constant of integration. Using Eq. (18) in Eqs. (7) and (8), we get,

$$\dot{\varepsilon}_r = -\frac{C}{r^2} \tag{19}$$

$$\dot{\varepsilon}_\theta = \frac{C}{r^2} \tag{20}$$

Under plane strain condition, Eq. (16) becomes,

$$\sigma_z = \frac{(\sigma_r + \sigma_\theta)}{2} \tag{21}$$

Substituting σ_z from Eq. (21) in to Eq. (17), we get,

$$\sigma_e = \frac{\sqrt{3}(\sigma_\theta - \sigma_r)}{2} \tag{22}$$

Substituting $\dot{\varepsilon}_r$ and σ_z respectively from Eqs. (19) and (21) into Eq. (14), we obtain,

$$\sigma_\theta - \sigma_r = \frac{1.33\sigma_e C}{\dot{\varepsilon}_e r^2} \tag{23}$$

Using Eqs. (4) and (22) in Eq. (23) and simplifying, one gets,

$$\sigma_\theta - \sigma_r = \frac{I_1}{r^{2/n}} \tag{24}$$

Where,

$$I_1 = \left[1.33\right]^{\frac{n+1}{2n}} \frac{C^{1/n}}{B^{1/n}} \tag{25}$$

Substituting Eq. (24) into Eq. (12) and integrating, we get,

$$\sigma_r = X_1 - p \tag{26}$$

Where,

$$X_1 = \int_a^r \frac{I_1}{r^{\frac{n+2}{n}}} dr \tag{27}$$

Substituting Eq. (26) into Eq. (24), we obtain,

$$\sigma_\theta = X_1 + \frac{I_1}{r^{2/n}} - p \tag{28}$$

To estimate the value of constant *C*, needed for estimating I_1, the boundary conditions given in Eqs. (10) and (11) are used in Eq. (26) with X_1(Eq. 27) integrated between limits a to b. to get,

$$\int_a^b \frac{I_1}{r^{\frac{n+2}{n}}} dr - p = -q \tag{29}$$

Substituting the value of I_1 from Eq. (25) in to Eq. (29) and simplifying, we obtain,

$$C = \left[\frac{p - q}{X_2}\right]^n \tag{30}$$

Where,

$$X_2 = \int_a^b \frac{(1.15)^{\frac{n+1}{n}}}{r^{\frac{n+2}{n}} B^{\frac{1}{n}}} dr \tag{31}$$

Using Eqs. (21) and (22) into Eqs. (14) and (15), one obtains,

$$\dot{\varepsilon}_\theta = -\dot{\varepsilon}_r = \frac{\sqrt{3}\dot{\varepsilon}_e}{2} \tag{32}$$

The analysis presented above yields the results for isotropic FGM cylinder.

5. Numerical Scheme of Computation

Follows the procedure described in section 4 to begin the numerical computation, the vlaues of X_2 Eq. (31) is estimated by substituting the value of the Creep parameters B and *n* from Eqs. (5) and (6) respectively.To obtain the value of constant C by substituted the vlaue of X_2 in Eq.(30) and using this value in Eq.(25), the value of I_1 is obtained. By using this value of I_1 in Eq.(27), the value of X_1 is obtained.

After getting the value of X_1, the Stresses σ_r and σ_θ are obtained from Eqs. (26) and (28) respectively. Now, to estimate the distribution of axial stress σ_z, the value of σ_r and σ_θ are substituted in Eqs.(21).after obtaining the value of σ_r, σ_θ and σ_z, the values of σ_e and $\dot{\varepsilon}_e$ are calculated from Eqs. (22) and (4) respectively. Finally the strain rates $\dot{\varepsilon}_r$ and $\dot{\varepsilon}_\theta$ are calculated respectively from Eqs. (14) and (15).

6. Results and Discussion

According to the analysis of numerical calculation, the creep stresses and strain rates in different composite cylinders (Non-FGM cylinder, FGM Linear Cylinder and FGM Non-Linear Cylinder) are obtained, as mentioned in Table 2.

Table 2: Details of different composite cylinders

Cylinder	*m* (gradation index)	$V_{max.}$ (*vol. %*)	V_{avg} (*vol. %*)	V_{min} (*vol. %*)
Non-FGM (C1)	0	20	20	20
FGM Linear (C2)	1	25	20	16
FGM Non-Linear (C3)	2	25	20	12.14

6.1 Validation

Before discussing the results obtaining from the analytical study, it is necessary to check the accuracy of the procedure carried out. To achieve this task, the tangential stress in a cylinder for which the results are reported by the Chen *et al.*, 2007 [8]. The dimensions, operating pressure and creep parameters of the cylinder are listed in Table 3. The tangential stress obtained in the cylinder is compared with that reported by Chen *et al.*, 2007 [8] and a good agreement is observed in Fig. 2 between the result obtained in present study and those of Chen *et al.*, 2007 [8].

Table 3: data used for validation Chen *et al.*, 2007 [8]

Creep parameters:	**B_o=2.77 x 10^{-16} (MP^{-n}/h) and *n* = 3.75**
Grading index:	ϕ = 0.7
Operating Pressure	*p* = 50 *MPa and q*= 0 *MPa*

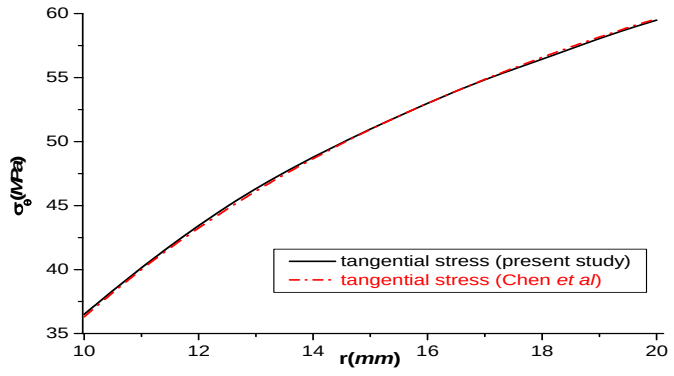

Fig 2: Validation of present study *vs* Chen *et al.,* 2007

6.1 *Variation of Creep Parameters*:

Figure 3 shows the variation of creep parameters *B* in different composite cylinders. In FGM cylinders (C2 and C3), the value of creep parameter B increases near the inner radius but its value decreases towards the outer radius and in Non-FGM cylinder (C1) the value of creep parameter B remains constant due to constant amount of SiC_P content.

Figure 4 shows the variation of creep parameters *n* with radial distance in different composite cylinders. In FGM cylinders (C2 and C3), the value of parameter *n* increases with increase in radius but for Non-FGM cylinder (C1) due to uniform amount of SiC_P (20 *Vol%*), it remains constant over the entire cylinder. The increase observed is due to lowering of SiC_P content in FGM cylinder (C2 and C3) with increasing radial distance. The variation of creep parameters *B* and *n* exhibits a crossover at a radius of around 16 mm.

Figure 5 shows the variation of reinforcement (SiC_P) in the different cylinders. It is observed that the distribution of reinforcement decreases linearly from inner to outer radius in FGM Linear cylinder (C2) while in FGM Non-Linear Cylinder (C3) decreases non-linearly from inner to outer radius. However, the Non-FGM Cylinder (C1) has uniform value because it remains 20% throughout. The value of FGM Non-Linear cylinder (C3) increases near the inner radius but decreases towards the outer radius when compared with the FGM Linear cylinder (C2) and Non-FGM Cylinder (C1).

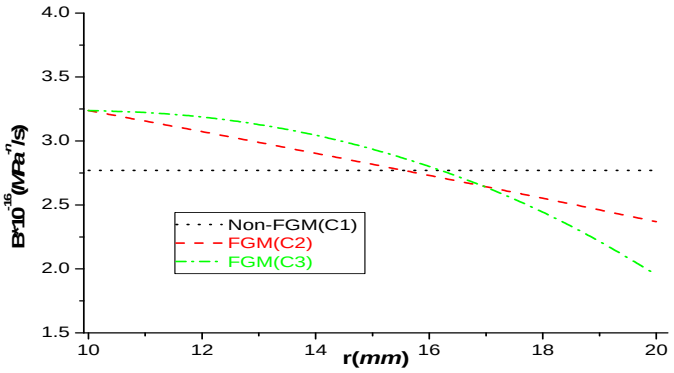

Fig 3: Variation of creep parameter *B* in cylinders

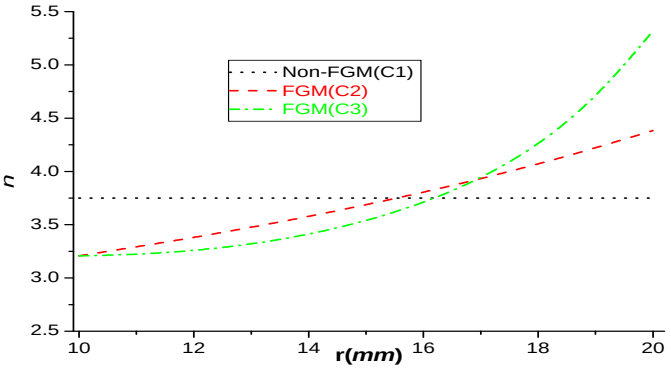

Fig 4: Variation of stress exponent *n* in cylinders

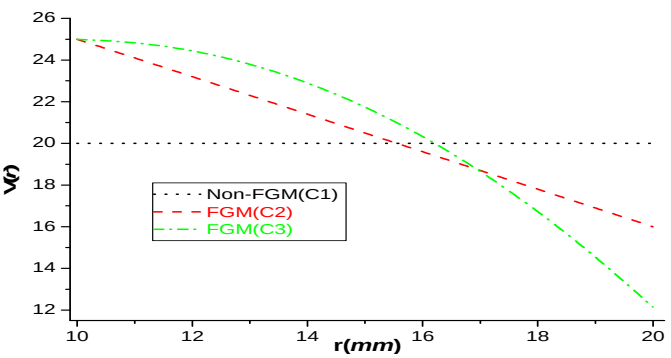

Fig 5: Variation of SiC_P Content in cylinders

6.2 Distribution of stresses and strains

Figure 6 shows the variation of radial stress in the different composite cylinders. It is observed that the radial stress remains compressive throughout the cylinder, with a maximum value at the inner radius and zero at the outer radius, under the imposed boundary conditions given by Eqs. (10) and (11). It is observed that the radial stress (compressive) decreases over the entire radius. The variation of radial stress in FGM cylinder is maximum than the Non-FGM Cylinder. In FGM Linear Cylinder (C2), the value of radial stress increases near the inner radius but decreases towards the outer radius when compared with the FGM Non-Linear Cylinder (C3).

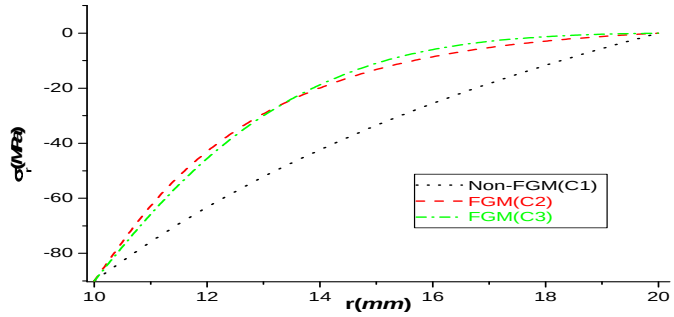

Fig 6: Variation of radial Stress in cylinders

Figure 7 shows the variation of tangential stress in the different composite cylinders. The tangential stress remains tensile throughout in all different composite cylinders and by observation in the Non FGM cylinder (C1), increases with increase in radius but by increasing Particle gradient in the FGM Linear (C2) and Non-Linear (C3) Cylinder, the tangential stress increases near the inner radius but decreases toward the outer radius. In Non-Linear FGM cylinder (C3), the tangential stress significantly increases by 120 *MPa* near the inner radius but decreases by 102 *MPa* near the outer radius as compared with the Non-FGM Cylinder (C1). The value of tangential stress in Non-Linear FGM cylinder (C3) is higher in the middle of the radius (12 *mm* to 16 *mm*) than the Linear FGM cylinder (C2). The variation of SiC_P Content exhibits a crossover at a radius of around 14 *mm* to 15 *mm.*

Figure 9 shows the variation of radial and tangential strain rates in the different composite cylinders. It is observed that the effect of radial and tangential strain rates in the cylinders decreases with increasing radius. The radial and tangential strains rates are the highest in Non-FGM cylinder (C1) and the lowest in FGM Non-Linear Cylinder (C3) when compared to FGM Linear Cylinder (C2). The magnitude of the radial and tangential strain rates in all composite cylinder are significantly higher near the inner radius but lower near the outer radius.

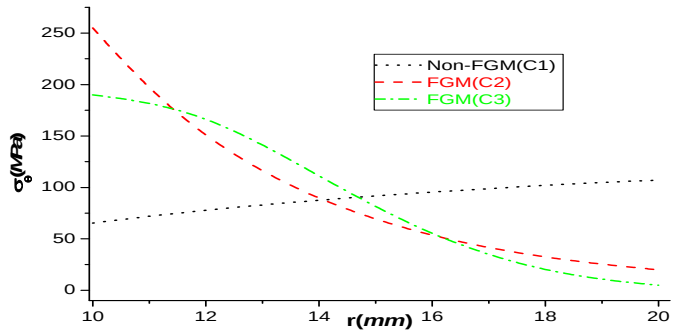

Fig 7: Variation of Tangential Stress in cylinders

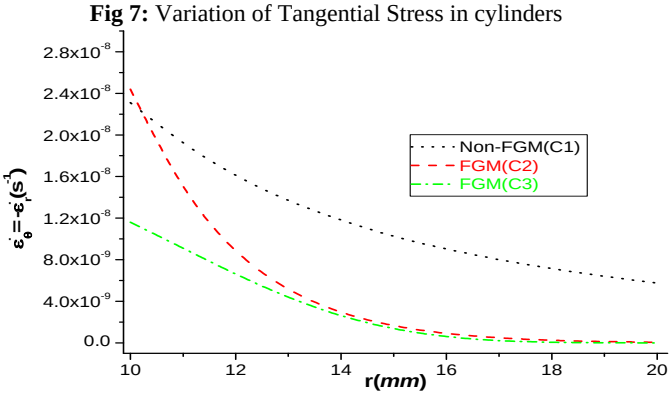

Fig 9: variation of radial and tangential strain rate in cylinders

7. Conclusions

The study carried out has led to the following conclusions:

1. The radial stress is compressive in the composite cylinder decreases throughout all the cylinders.
2. In the FGM Linear and FGM Non-Linear (C2 and C3) cylinders, the tangential and effective stresses decrease towards the outer radius due to decreasing of distribution of SiC_P reinforcement.
3. The strain rates (radial and tangential) in FGM Linear cylinder (C2) lie in between the values obtained for Non-FGM cylinder (C1) and FGM Non-Linear Cylinder (C3).
4. The strain rates in the composite cylinder reduce significantly in the presence of non-linear SiC_P gradient.

8. References

1. Arya VK, Bhatnagar NS. “Creep of thick walled orthotropic cylinders subjected to combined internal and external pressures”, Journal of Mechanical Engineering Science, 1976; 18(1):1-5
2. Arya VK, Debonath KK, Bhatnagar NS. “Creep analysis of orthotropic cylindrical shells”, International Journal of Pressure Vessels and Piping 1983; 11(3):167-190.
3. Becht, IV C, Chen Y. “Span limits for elevated temperature piping” Journal of Pressure Vessel Technology 2000; 122(2):121-124
4. Bhatnagar NS, Gupta SK. “Analysis of thick-walled orthotropic cylinder in the theory of creep”, Journal of the Physical Society of Japan 1969l; 27(6):1655-1662.
5. Bhatnagar NS, Arya VK, Debonath KK. “Creep analysis of orthotropic rotating cylinder”, Journal of Pressure Vessel Technology 1980; 102(4):371-377.
6. Birman V, Byrd LW. “Modeling and Analysis of Functionally Graded Materials and Structures”, Applied Mechanics Reviews 2007; 60(5):195-216
7. Chen W, Gui-ru YE, Jin-biao CAI. “Themoelastic stresses in a uniformly heated functionally graded isotropic hollow cylinder”, Journal of Zhejiang University Science 2002; 3(1):1-5.
8. Chen JJ, Tu ST, Xuan FZ, Wang ZD. “Creep analysis for a functionally graded cylinder subjected to internal and external pressure”, Journal of Strain Analysis of Engineering Design 2007; 42(2):69-77.
9. Dieter GE. “Mechanical Metallurgy”, 3rd ed. London, McGraw-Hill Publications, 1988.
10. Hagihara S, Miyazaki N. “Finite element analysis for creep failure of coolant pipe in light water reactor due to local heating under severe accident condition”, Nuclear

Engineering Design 2008; 238(1):33-40.
11. Gupta SK, Pathak S. “Thermo creep transition in a thick walled circular cylinder under internal pressure”, Indian Journal of Pure and Applied Mathematics 2001; 32(2):237-253.
12. Loghman A, Ghorbanpour AA, Aleayoub SMA. “Time-dependent creep stress redistribution analysis of thick-walled functionally graded spheres”, Mechanics of Time-Dependent Materials 2011; 15:353-365.
13. Obata Y, Noda N. Steady thermal stresses in a hollow circular cylinder and hollow sphere of a functionally graded materials, Journal of Thermal Stresses 1994; 17(3):471-487.
14. Singh SB, Ray S. “Steady-state creep behavior in an isotropic functionally graded material rotating disc of Al-SiC composite”, Metallurgical and Materials Transactions 2001; 32(7):1679-1685.
15. Singh T, Gupta VK. “Effect of anisotropy on steady state creep in functionally graded cylinder”, Composite Structures 2011; 93(2):747-758.
16. Tachibana Y, Iyoku T. “Structural design of high temperature metallic components”, Nuclear Engineering and Design 2004; 233(1-3):261-272.